

# Entropic Tightening of Vibrated Chains

M. B. Hastings<sup>1,2</sup>, Z. A. Daya<sup>2,3</sup>, E. Ben-Naim<sup>1,2</sup>, and R. E. Ecke<sup>2,3</sup>

<sup>1</sup>Theoretical Division, <sup>2</sup>Center for Nonlinear Studies, <sup>3</sup>Condensed Matter & Thermal Physics Group  
Los Alamos National Laboratory, Los Alamos, NM 87545

(October 15, 2001)

We investigate experimentally the distribution of configurations of a ring with an elementary topological constraint, a “figure-8” twist. Using vibrated granular chains, which permit controlled preparation and direct observation of such a constraint, we show that configurations where one of the loops is tight and the second is large are strongly preferred. This agrees with recent predictions for equilibrium properties of topologically-constrained polymers. However, the dynamics of the tightening process weakly violate detailed balance, a signature of the nonequilibrium nature of this system.

PACS: 05.40.-a, 81.05.Rm, 83.10.Nn

Topological constraints such as knots and entanglements constantly form and relax in polymer systems and in biomolecules such as DNA [1–6]. These constraints increase relaxation time scales and additionally restrict the phase space accessible by the macromolecule. Whereas the role entanglements play in chain dynamics is well appreciated [7,8], even more basic questions concerning effects of topological constraints on static properties such as the chain structure remain largely unanswered. Recent theoretical studies predict that in equilibrium, a knotted polymer will generally favor configurations where the knot is “tight”, *i.e.*, localized to a small region of the chain [9,10]. Numerical simulations and scaling analysis support this prediction [11], but direct experimental tests are difficult [12]. In this study, we examine this interesting prediction experimentally using vertically vibrated granular chains.

Granular chains consist of spherical beads connected by rods, and their backbone enforces the same geometrical constraints as in a polymer system. A vibrating plate supplies the system with energy, balancing the energy dissipation due to inelastic collisions experienced by beads [13–16]. This polymer system is well suited for studying topological constraints as it allows control of the chain size and the constraint type, as well as direct observations of the chain conformation in contrast with traditional polymer systems. Recent studies have successfully used vibrated chains to study diffusive relaxation [17] and spontaneous formation [18] of knots.

We considered the simplest possible topology, a “figure-8”: a once-twisted ring consisting of two loops, separated by a single crossing point, which functions as the topological constraint (see Fig. 1). Under appropriate vibration amplitude, the system is effectively two-dimensional and the crossing point hops along the chain without flipping open the figure-8. Surprisingly, despite the highly nonequilibrium drive applied to the system, we observed strong entropic tightening. The microscopic degrees of freedom, the beads, experience periodic drive and dissipative collisions with the plate, rods, and other beads, as well as frictional forces. Remarkably the macro-

scopic observable, the loop size, obeys a statistical mechanics. Detailed balance is only weakly violated and the empirical loop-size distribution is close to that conjectured on entropic grounds. This provides an opportunity for studying the role of entropy in nonequilibrium systems. We now review the equilibrium result for the loop-size distribution.

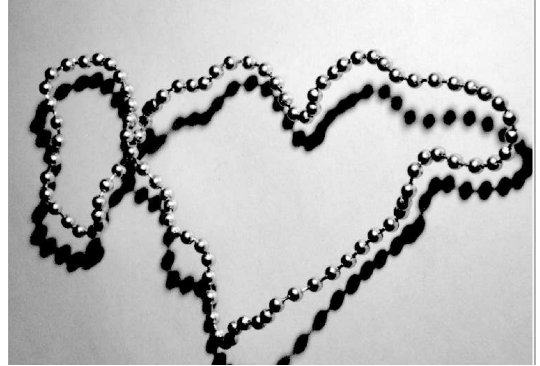


FIG. 1. A vibrated ring with a figure-8 twist.

Tightening of knots in polymers can be understood by considering the simplest case, in which electrostatic interactions are perfectly screened. Suppose a knot in the polymer can be considered as located at a point, with several loops of lengths  $N_1, N_2, \dots$  projecting from the knot. Ignoring hard-core interactions, each loop has a linear size of order  $N_i^{1/2}$ , so that the number of configurations in which the chain returns to itself and forms a loop is proportional to  $e^{cN} \prod_i N_i^{-d/2}$ , where  $d = 2$  is the spatial dimension, and  $c$  is a constant. Therefore, assuming all microscopic configurations are equally likely, the probability of having a given  $N_1, N_2, \dots$  is maximized when  $N_1 \approx N$  and  $N_2, \dots$  are all as short as possible. That is, the knot spontaneously tightens due to entropic effects.

A ring with a figure-8 constraint is natural for studying this effect as it simply contains two loops of sizes  $N_1, N_2$  with the overall size  $N = N_1 + N_2$  fixed. The argument above predicts a power law divergence in the loop-size probability distribution

$$\rho(n) \propto n^{-\alpha} \quad (1)$$

with  $n \equiv N_1, N_2$  for  $1 \ll n \ll N$ . The exponent  $\alpha = 43/16 \approx 2.7$  can be obtained even when excluded volume interactions are taken into account [11,19]. Although this is obtained from large  $n, N$  asymptotics, an enumeration for smaller sizes only leads to small corrections to this form.

Our apparatus consists of an anodized aluminum plate, driven sinusoidally by an electromechanical vibrator. The bead and rod chains consist of hollow nickel-plated stainless steel spheres of radius  $1.18 \pm 0.01$  mm connected by thin rigid rods of radius  $0.26 \pm 0.01$  mm. The rods constrain both the bending and stretching of the chain. In particular, the rods must lie within a cone of a half-angle of roughly  $25^\circ$  about the axis of either of the two adjacent rods, and the separation  $b$  between two adjacent beads lies in the range  $0 \leq b \leq 0.94$  mm. The chains were connected end-to-end to form rings, and then twisted with a single crossing point thereby forming a figure-8. For the experiments reported here, the number of beads in the figure-8 ring was between 69 and 219, much larger than the tightest possible 8-bead loop. The plate was oscillated harmonically at a frequency of 16 Hz.

The dynamics of the crossing depend on the rms acceleration of the plate,  $\gamma$  (this dimensionless quantity is in units of the gravitational acceleration  $g$ ). For  $\gamma \lesssim 1.35$ , the crossing does not move along the chain. For  $\gamma \gtrsim 1.55$ , the vertical motion of the chain is large enough that the number of crossings in the ring is not fixed: a loop of the figure-8 can easily flip, untwisting the ring, or creating additional crossings. We chose  $\gamma = 1.5$ , for which flipping events remained rare, occurring every roughly  $10^4$  oscillation cycles, while the crossing remained mobile, with approximately 50% chance of the loop size changing in a 1/16-th second cycle. In Fig. 2 we show the distribution of change in loop size in one cycle. The acceleration was constant and uniform across the plate to better than 1%. The 27.2 cm plate diameter, corresponding to approximately 115 beads, was large enough so that collisions with the sloped acrylic wall were rare.

Digital images of the chain were obtained to determine the loop size distribution. Image analysis requires a two step procedure involving: (i) monomer recognition, and (ii) chain reconstruction. To obtain the monomer positions, images of resolution  $1000 \times 1016$  pixels were acquired. At this resolution, the reflected light from a bead appears in the images as a bright spot of about  $5 \times 5$  pixels, even though the bead has a diameter of just over 8 pixels. The positions of the beads were determined by fitting the intensity pattern generated by each bead to a Gaussian, with the peak position taken as the bead position. We estimate the positional accuracy obtained using this procedure as 0.05 bead diameters.

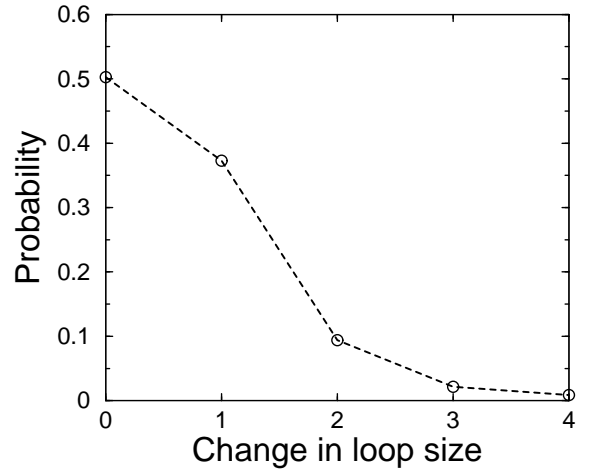


FIG. 2. Distribution of absolute change in loop size over 1/16-th second, showing the rapidly decreasing probability of larger jumps.

Given these positions, the order of the monomers along the chain was determined using an efficient greedy algorithm which requires only  $N^2$  operations for an  $N$ -bead ring. This algorithm utilizes the aforementioned geometrical restrictions on stretching and bending imposed by the rods (given two connected beads, the third was searched only in a properly restricted neighborhood). Once the ring was reconstructed, the crossing point was identified, thereby determining the loop sizes.

We first sampled the loop size at a much slower rate of 0.25 Hz. Starting with two equal-size loops at each run for a chain of size  $N = 149$ , we obtained the loop-size distribution shown as the inset to Fig. 3. This distribution has a sharp peak located at the smallest possible loop size. Hence, the conjectured tightening is indeed observed. We repeated the experiments using larger beads, changing the driving frequency to 13 Hz, and using chains of length 49, 69, 99, and 219, as well as using a plate with different roughness. Further, many sets of images at arbitrary phase with respect to the driving were analyzed. In all these cases, the same qualitative loop-size distribution emerged. There were, however, some quantitative differences with the peak height varying by about 20%. Since the number of hopping events before flipping is of the same order as  $N^2$  ( $\sim 10^4$ ), the flipping introduces a dependence on the initial conditions, which is more pronounced for the longer chains. Even worse, flipping events typically occur when the loops are small, leading to a reduction of the peak height. Therefore, we used an alternate method of determining the loop size distribution.

To find the true peak height, *with flipping events removed*, we measured the loop size at a much faster frame rate of 16 Hz, and experimentally determined the transition probability  $t_{i,j}$  from a loop of size  $i$  to a loop of size  $j$ . To sample  $t_{i,j}$  for all  $i$ , the twisted ring was started

manually at various equally-spaced loop sizes, and then allowed to run for 200 cycles to let the chain equilibrate, after which 200 frames were taken to measure  $t_{i,j}$ . By taking 20,000 total frames over 100 separate runs, we obtained an accuracy of 10% on individual  $t_{i,j}$ . After equilibration, correlations between successive transitions were negligible, implying a Markov process.

Given Markovian dynamics, it is possible to calculate the steady state probability,  $\rho_i$ , of the loop having size  $i$ , from the  $t_{i,j}$  by performing a Monte Carlo simulation of the transition process. For a chain of length 149, we found the distribution shown as the solid line in Fig. 3. Compared to that measured directly, this histogram is characterized by a sharper peak and considerable curvature at the center because flipping events and dependence on initial conditions were eliminated, respectively. The dashed line shows the theoretical curve  $\rho_i \propto [i^{-\alpha}(N-i)^{-\alpha}]$ , with  $\alpha = 43/16$ . The two curves are consistent, although the peak is more sharply defined in the solid line. Making quantitative statements about the relation between the curves would require much larger chain lengths  $N$  to obtain a sufficient scaling region. Further, the statistical error in  $\rho_i$  is most pronounced in the center of the histogram where  $\rho_i$  is small. Other chain lengths have similar histograms, in this case using 0.25 Hz transition rates.

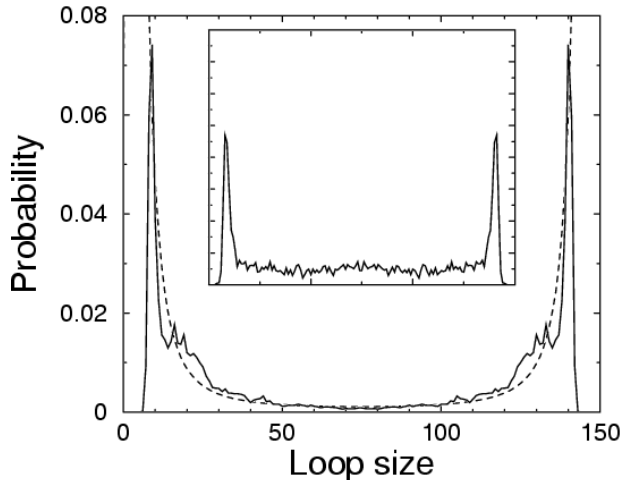


FIG. 3. Loop-size distribution obtained from transition rates (solid line), and equilibrium result (dashed line). Inset: Loop-size distribution from direct observation, with same scale as main figure.

The transition rates enable us to check detailed balance, a sharp test of the nonequilibrium nature of the system. For a system in thermal equilibrium, detailed balance implies a vanishing net flux between any two microscopic states, namely  $\rho_i t_{i,j} = \rho_j t_{j,i}$ , or  $f_j(i) \equiv \ln[(\rho_i t_{i,i+j})/(\rho_{i+j} t_{i+j,i})] = 0$ . Interestingly, we have found that  $f_1(i) > 0$  and  $f_2(i) < 0$ , namely, short jumps tend to tighten the loop more than long jumps.

This is shown in Fig. 4, where we plot a moving average of  $f_1(i)$  as the solid line, and a moving average of  $f_2(i)$  as the dashed line. The average of  $f_1(i)$  is  $0.1 \pm 0.02$  for  $i > 100$ .

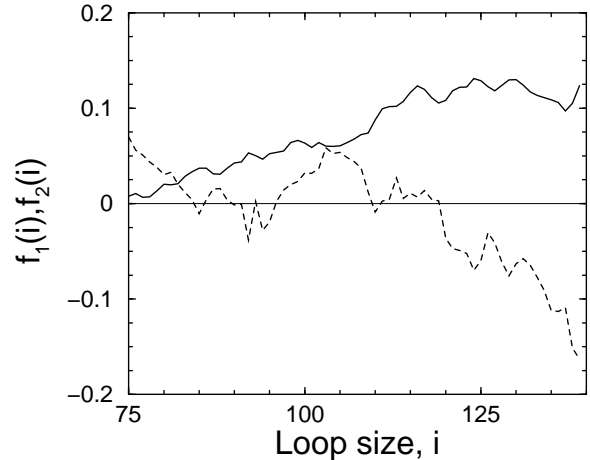


FIG. 4. Plot of smoothed  $f_1(i)$  (solid line), and smoothed  $f_2(i)$  (dashed line).

As this is an important point, we have made several additional checks. We also considered  $f_1(i) + f_1(i+1) - f_2(i+2)$ , which measures the flux around a three point neighborhood. This  $\rho$ -independent quantity was positive, demonstrating violation of detailed balance directly from the  $t_{i,j}$ . Furthermore, we tested detailed balance using 0.25 Hz transition rates for other chain lengths, and again found that short jumps tighten the loop more than long jumps. As a final check, we have tested this procedure using surrogate data from a simulated process which satisfies detailed balance to verify that the violation is not an artifact of the reconstruction of  $\rho$  from the  $t_{i,j}$ .

Since it is surprising that an argument based on counting of states should be relevant in a nonequilibrium system, we now consider a simplified model. We show that, even out of equilibrium, there are entropic tightening forces, despite violation of detailed balance and possible quantitative changes in the size distribution. We consider a chain with linear elastic interactions between neighboring beads and ignore self-avoidance. We will first consider the equilibrium case, with the chain subject to thermal forcing and damping, and then generalize to athermal drive. Number the beads from 1 to  $N$ , and label the position of bead  $i$  by  $\vec{x}(i)$ . Let the crossing occur at beads  $n_1, n_1 + 1$  and  $n_2, n_2 + 1$ . We will compute the forces on the crossing, and from this derive an effective dynamics.

Assume  $n_1 < n_2$ , and consider the loop formed by beads  $n_1 + 2, n_1 + 3, \dots, n_2 - 2$ . This loop exerts a force on bead  $n_1 + 1$  proportional to  $\vec{x}(n_1 + 2) - \vec{x}(n_1 + 1)$ . This force tries to tighten the loop. Summing over normal modes of the loop, the average force of a loop of length  $n$  is found to be  $kT(c-1/n)$ , with  $c > 0$ . The fluctuations in

this force introduce an effective noise into the dynamics of  $n_1$ . There is also an effective dissipation: if the crossing moves to tighten a given loop, the force exerted by that loop temporarily increases (both these contributions are determined by short distance effects). We then make an approximation that  $n_1, n_2$  can be treated as particles of mass  $M$  subject to the above forces. The resulting dynamics for  $n = n_2 - n_1$  when  $n \ll N$  is,

$$M\partial_t^2 n = -\frac{kT}{n} - \nu\partial_t n + \eta(t), \quad (2)$$

where  $\nu$  is the dissipation parameter and  $\eta$  is the noise. By the fluctuation-dissipation theorem, noise and dissipation in (2) are such that  $n$  also behaves as a thermal particle at temperature  $T$ , giving an equilibrium distribution  $\rho(n) \propto n^{-d/2}$ .

Suppose instead that the chain is subject to forcing which is athermal with large, non-Gaussian fluctuations at short distances, a reasonable assumption given the collisions with the plate. One can show that the average force remains proportional to  $-1/n$ , but the noise in (2) also becomes athermal. The effect of this is most easily understood in the overdamped limit of (2). Then,  $n$  executes a biased random walk with a drift of order  $1/n$  [20], with additional random jumps of varying size due to noise. As a result, large jumps are relatively less biased compared with small jumps, and detailed balance is violated as in the experiment. At large  $n$  this gives biased diffusion, with the diffusivity determined by the mean-square step size. This yields  $\rho \propto n^{-\alpha}$ ,  $\alpha \neq d/2$ . For smaller  $n$ , the probability distribution is determined only by the smaller jumps which are more biased, giving a sharpening of the peak in the distribution at a width of the order of the largest jump size, consistent with observations. This behavior is independent of the precise form of the noise, as confirmed by our numerical simulations of (2).

Finally, we consider the dynamics of constraints in linear chains instead of rings. In this case, knots can open at the ends of the chain. Consider a linear chain which crosses itself at one point, the analogue of the figure-8 considered here. Let the crossing occur at links  $n_1, n_2$ , with  $0 < n_1 < n_2 < N$ . The points  $n_1, n_2$  describe a random walk, with boundary conditions  $n_1 < n_2$ , and a bias proportional to  $1/(n_2 - n_1)$ . For  $\alpha > 1$ , the two walkers form a bound state, and the time for the knot to open will behave for large  $N$  as for a single random walker. This contrasts with the behavior found in a larger acceleration regime, for which experimental measurements of knot opening times showed a purely diffusive behavior [17], with negligible entropic interaction between walkers. We speculate that the reason for the reduced interaction in the larger acceleration regime is that the increased drive takes the system further out of equilibrium.

In conclusion, we have observed a spontaneous tightening of topological constraints in vertically vibrated gran-

ular chains. The significance of this phenomenon is that it indicates that the presence of the constraint merely reduces the chain length by a fixed amount, rather than leading to an extensive size reduction. For equilibrium polymers the tightening arises from entropy. Here, due to the strongly nonequilibrium drive applied to the system, the bead dynamics is athermal and the crossing dynamics breaks detailed balance. However, the loop-size distribution remains close to equilibrium. This system provides further possibilities for experimental examination of the role of entropic forces in nonequilibrium statistical mechanics. It is possible to probe fluctuation-dissipation relations by a quantitative comparison between the forces on the crossing point and the velocity fluctuations in the beads, namely the granular temperature.

We thank Charles Reichhardt for useful discussions. This work was supported by US DOE(W-7405-ENG-36) and by the Canadian NSERC.

- 
- [1] S. Nachaev, *Statistics of Knots and Entangled Random Walks* (World Scientific, Singapore, 1996).
  - [2] H. L. Frish and E. Wasserman, *J. Am. Chem. Soc.* **83**, 3789 (1961).
  - [3] D. W. Sumners and S. G. Wittington, *J. Phys. A* **21**, 1689 (1989).
  - [4] S. Y. Shaw and J. C. Wang, *Science* **260**, 533 (1993).
  - [5] S. R. Quake, *Phys. Rev. Lett.* **73**, 3317 (1994).
  - [6] E. Ben-Naim, G. S. Grest, T. A. Witten, and A. R. C. Baljon, *Phys. Rev. E* **53** 1806, (1996).
  - [7] P. G. de Gennes, *Scaling Concepts in Polymer Physics* (Cornell, Ithaca, 1979).
  - [8] M. Doi and S. F. Edwards, *The Theory of Polymer Dynamics* (Clarendon Press, Oxford, 1986).
  - [9] V. Katrich, W. K. Olson, A. Vologodskii, J. Dubochet, and A. Stasiak, *Phys. Rev. E* **61**, 5545 (2000).
  - [10] A. Yu. Grosberg, *Phys. Rev. Lett.* **85** 3858 (2000).
  - [11] R. Metzler, A. Hanke, P. G. Dommersnes, Y. Kantor, M. Kardar, cond-mat/0110266.
  - [12] S. R. Quake, H. Babcock, and S. Chu, *Nature* **388**, 151 (1997).
  - [13] L. P. Kadanoff, *Rev. Mod. Phys.* **71**, 435 (1999).
  - [14] H. Jaeger, S. Nagel, and R. P. Behringer, *Rev. Mod. Phys.* **68**, 1259 (1996).
  - [15] J. S. Olafson and J. S. Urbach, *Phys. Rev. Lett.* **81**, 4369 (1998).
  - [16] F. Mello, P. B. Umbanhowar, and H. L. Swinney, *Phys. Rev. Lett.* **75**, 3838 (1995).
  - [17] E. Ben-Naim, Z. A. Daya, P. Vorobieff, and R. E. Ecke, *Phys. Rev. Lett.* **86**, 1414 (2001).
  - [18] A. Belmonte, M. J. Shelley, S. T. Eldakar, and C. H. Wiggins, *Phys. Rev. Lett.* **87**, 114301 (2001).
  - [19] B. Duplantier and S. Saleur, *Phys. Rev. Lett.* **57**, 3179 (1986).
  - [20] B. D. Hughes, *Random Walks and Random Environments, Vol. 1*, (Clarendon Press, Oxford, 1995).